Mechanical and Corrosion Behaviour of Dissimilar AA2024–AA3003 Aluminum Matrix Composites Reinforced with TiC and ZrC Joined by Friction Stir Welding

Prabhu L[1*], *Kevin* George[2], *Saravanan* M[3] , *Selvababu* B[3]

[1]Professor, Department of Mechanical Engineering, Aarupadai Veedu Institute of technology, Vinayaka Mission's Research foundation, Salem, TamilNadu
[2]PG Scholar,Department of Mechanical Engineering, Aarupadai Veedu Institute of technology, Vinayaka Mission's Research foundation, Salem, TamilNadu
[3] Assistant Professor, Department of Mechanical Engineering, Aarupadai Veedu Institute of technology, Vinayaka Mission's Research foundation, Salem, TamilNadu

Abstract. Aluminum was a highly favored material because of its affordability, lightweight nature, excellent formability, and ease of machinability. The incorporation of non-metal, like ceramics, into aluminum alloys results in the formation of composite materials. Metal Matrix Composites are being developed as substitutes for traditional metals owing to their capacity to endure substantial loads, superior resistance to wear and corrosion, and relatively high toughness and hardness. The results showed that ultimate tensile strength (UTS) of AA3003 alloy welded with AA2024/5% TiC was the highest at 140.82 MPa, while the lowest UTS was observed in the AA2024/5% ZrC welded with Al 3003/5% TiC at 88.06 MPa. In terms of hardness, the highest Brinell Hardness Number (BHN) of 74.25 was observed in the Al 3003/5% ZrC welded with Al 2024/5% ZrC. Regarding corrosion resistance, the specimens with alumina reinforcement showed the best performance, with acidic corrosion rates (CR_A) as low as 0.8 mpy and basic corrosion rates (CR_B) as low as 0.57 mpy for AA2024/5% TiC welded with AA3003/5% TiC. Aluminum Matrix Composites were the predominant category under Metal Matrix Composites (MMCs) appealing characteristics, including elevated hardness, high strength-to-weight ratio, exceptional tribological performance, and significant impact strength, facilitate their application in automotive components, aerospace structures, and maritime parts. This research endeavors to synthesize Aluminum Matrix Composites (AMC) and Aluminum Alloys via the widely employed synthesis method known as stir casting, followed by joining them through friction stir welding. Different grades of aluminum alloy, specifically AA 2024 and AA 3003, are utilized for experimental work. Alumina and zirconium carbide serve as reinforcements within the aluminum matrix. MCDM numerical optimization method, specifically the Multi-Attribute Border Approximation Area comparison (MABAC) and the Criteria Importance Through Intercriteria Correlation (CRITIC), with a coefficient of 0.01 (combination of AA2024/5% TiC welded with AA3003/5% TiC),

* Corresponding author:prablogu@gmail.com

was used, making it the best solution for achieving the best balance between mechanical properties and corrosion resistance.

1.Introduction

An alloy is a combination of more metals in defined ratios. Typically, all metals are found in alloys. Aluminum, predominant metal in Earth's crust, is derived from bauxite ore and refined into alloy. Sustainability evaluation of FSW for metal-plastic hybrid joints reveals that self-piercing riveting (SPR) outperforms both FSW and adhesive bonding, offering better overall sustainability in environmental, social, and economic factors [1]. Friction stir welding of AA2024-T351 showed that FSW outperformed MIG and TIG in tensile strength, with FSW joints exhibiting significantly improved weld quality, hardness, and tensile properties [2]. Friction stir welding of dissimilar AA2024 and copper with a cylindrical pin tool revealed that optimal parameters increased tensile strength, microhardness, joint efficiency, and elongation, with the best results at 900 rpm [3]. Friction stir welding of AA3003 alloy pipes optimized at 900 rpm and 131.94 mm/min traverse speed improved tensile strength, microhardness, and impact energy, with a 38% increase in impact energy over base metal [4]. The effect of pin eccentricity in FSW of AA2024, showing that an eccentric square pin enhances mechanical properties, weld efficiency, and microstructure, offering a defect-free, high-performance aluminum matrix composite [5]. Post-weld heat treatment of nano-grained AA2024 FSW joints improved tensile strength and ductility, with the Orowan looping mechanism enhancing the microstructure, proving FSW's effectiveness in aluminum matrix composites [6]. The impact of different pin profiles on AA2024 in FSP showed that threaded pin tools, particularly tapered cylindrical threaded tools, improve grain refinement, hardness, and tensile strength, enhancing toughness and impact strength in aluminum matrix composites [7]. AA2024 and AA7075 showed that the RD∥45° welding combination enhanced material flow, tensile strength, and mechanical properties, improving toughness and corrosion resistance in aluminum matrix composites [8]. FSW of AA2024-T3 and SS304 dissimilar joints improved tensile strength, wear resistance, and corrosion resistance, demonstrating the potential of optimized welding conditions for high-performance aluminum matrix composites[9]. AA3105/AA2024 dissimilar FSW highlighted the influence of welding parameters on mechanical properties and residual stresses, showing potential for improving toughness and corrosion resistance in aluminum matrix composites [10]. Heat input during friction stir welding of AA2024 and A390-10 wt.% SiC composite joints enhanced stir zone mixing and particle distribution, improving strength, hardness, and corrosion resistance, with maximum properties at lower heat inputs [11]. Corrosion resistance of AA3003 FSW joints in aggressive media was improved with the inclusion of ethylene glycol, reducing corrosion rates and enhancing crack propagation resistance [12]. FSW joints of AA3003 exhibited lower corrosion rates compared to base metal, with ethylene glycol enhancing protection and delaying crack propagation in aggressive media [13]. Hybrid MCDM (Multi criteria Decision Model)-PSO techniques optimize FSW parameters for AA2024 and brass plates, with the preference ranking organization method for enrichment evaluation combined with PSO delivering superior performance and significant computational time savings [14]. CARCACS, a novel hybrid MCDM methodology, effectively ranks alternative solutions in decision-making. Applied to FSW tool material selection, it consistently identifies H13 tool steel as the best choice with reliable results [15]. TOPSIS and EWM optimize machining factors for AA2024/nZrO2 composites in squeeze casting, emphasizing process control to enhance wear resistance and ensure material consistency [16]. Optimization of underwater friction stir welding (UFSW) for SiC-reinforced A356

aluminum shows significant improvements in tensile strength, elongation, and yield strength using MCDM techniques. Optimal parameters resulted in defect-free welds with superior mechanical properties [17]. Ball milling AA7178 with ZrSiO4 nanoparticles and hot pressing enhanced mechanical properties, with uniform nanoparticle distribution improving strength, while excessive reinforcement led to property degradation [18]. Wear resistance of AA5052/B4C composites improved with increasing reinforcement volume and particle size ratio, but excessive reinforcement caused particle breakage, reducing wear resistance [19].This research use MADM to determine the ideal combination of the FSW method due to the discontinuous character of the findings acquired from numerous testing. An analysis of diverse literature about the FSW of aluminum matrix composites (AMCs) and aluminum alloys indicates FSW were only performed on alloy–alloy combinations and composite–composite, utilizing similar ceramic at both plates. To rectify deficiency, effort undertaken to manufacture and study friction stir welding (FSW) at alloy-composite and composite-composite combinations, using various ceramics at side plates. Composites and dissimilar aluminum alloys were bonded using friction stir welding (FSW). The corrosion resistance of welds is subjected to experimental analysis. The experimental methods employed for the fabrication and processing of the composites. The experimental results presented systematically. The results of corrosion and mechanical tests were presented and meticulously examined here. Multi-criteria decision-making problem is introduced and resolved systematically. Ultimately, concise results are derived from the experimental and MCDM simulations.

2.Methodology

2.1. Materials

The initial prerequisite for constructing welding is selection of materials for both the matrix and reinforcement. This portion of the article addresses acquisition and selection of raw materials.

(a) Matrices
The matrix is a component that envelops and supports the composite structure. AMC were inherently an aluminum alloy with the highest percentage. Elemental Analysis of the chosen two aluminum alloy, AA 2024 and AA 3003 is mentioned in Table1 and Table2.
AA 2024 were predominant and widely utilized aluminum alloy, characterized by substantial proportions of zirconium and magnesium.

Table 1. Elemental analysis of AA 2024

Constituents	**Si**	**Cr**	**Cu**	**Mg**	**Mn**	**Fe**	**Al**
Percentage	0.5	0.05	3.5	1.2	0.15	0.10	95.5

Table 2. Elemental analysis of AA3003**.**

Constituents	**Si**	**Cr**	**Cu**	**Mg**	**Mn**	**Fe**	**A1**
Percentage	0.6	0.05	0.05	0.05	1.0	0.3	98.5

(a) Reinforcements

Reinforcement material in minimal proportions were incorporated into metallic matrix as powder, whisker or a fiber. It imparts adhesive strength to the composite. This study is about two prominent ceramics, titanium carbide (TiC) and zirconium carbide (ZrC), as reinforcements. These ceramics are synthetic, exhibiting excellent abrasion characteristics and heat resistance as shown in Table 3.

Table 3. Properties of fillers.

Properties	**Titanium carbide (TiC)**	**Zirconium Carbide (ZrC)**
Coefficient of thermal expansion	9.5×10^{-6}	4.5×10^{-6}
Thermal conductivity	25	130
Tensile strength	220	140
Elastic modulus	320	420
Fracture toughness	5.2	4.9
Vickers hardness	1700	4500
Melting point	3000	2800
Density	4.10	3.60

2.2. Fabrication of the composites

This procedure involves melting metal alloy and casting it into the desired form. The metal designated for melting were placed into a graphite crucible and positioned into coal-fired furnace. The furnace combustion were regulated by mechanical blower. Aluminum alloys attain the liquidus phase or semi-solid state, warmed ceramic powders were introduced into molten metal and extensively agitated to guarantee uniform dispersion of reinforcing particles within matrix. Inadequate agitation lead to accumulation of ceramic particles residue at base of the crucible. The liquid were subsequently poured at mold cavity of the desired form and dimensions. The current research involves mild steel. Upon solidification, cast composite were extracted from die and subjected to air quenching.

Required Volume $= 15 \times 15 \times 0.5 = 112.5\text{cm}^3$;

Density of $\text{AA2024} = \text{AA3003} \approx 2.7\text{gm}/\text{cm}^3$;

Required mass $= 2.7 \times 112.5 = 303.75\text{gm}$;

Density = mass/volume;

Casting allowance $= 15\%$ of mass;

Therefore, the ultimate needed mass of metal is 303.75 g + (0.15 × 303.75 g) = 349.31 g.

An increase at the percentage of metal alloy augment dimensions or size of composite. To achieve the desired form, the percentage of the metal alloy must not be diminished in terms of volume-based ratio. A decrease in the percentage of metal alloy will lead to an unfinished casting form. The incorporation of reinforcement powders will augment the

composite's weight, as both ceramics possess more density than two distinct grades of aluminum. The mix of composites and alloys produced by stir casting were detailed below in Table 4.

Table 4: Material Combinations and Reinforcement Weights

Material Combination	Weight of Material (gm)	Weight of Reinforcement (gm)
100% AA2024	350	-
100% AA3003	350	-
100% AA2024 + 5% TiC	350	17.5
100% AA3003 + 5% TiC	350	17.5
100% AA2024 + 5% ZrC	350	17.5
100% AA3003 + 5% ZrC	350	17.5

2.3. Processing Technique

This section briefs the process of uniting the composite plates using FSW. Friction Stir Welding is one of the primary method employed to unite two plates composed of aluminum composites or aluminum alloys. The alloy plates or composite, designated for welding are positioned at close proximity, ensuring longitudinal edges make contact. The complete work-holding apparatus is positioned in the vertical milling machine. Holder consists of cylindrical tool fabricated from stainless steel, with a height and nose tip radius of 3 mm and 4 mm, with a diameter of 15 mm. Upon contact between revolving tool and stationary plates, welding action occurs at joints of two plates, induced by heat generated from friction, fusing together. Table 5 delineates the process parameters employed in FSW. Fig. 1 illustrates a collection of plates connected by FSW

Table 5. Parameters at Friction Stir Welding.

Parameters	Ranges
Tool pin nose radius	3
Tool material	Stainless steel
Tool pin shape	Cylindrical
Direction of tool rotation	Clock-wise
Traverse feed	50 mm/min
Tool MMC	1000 rpm

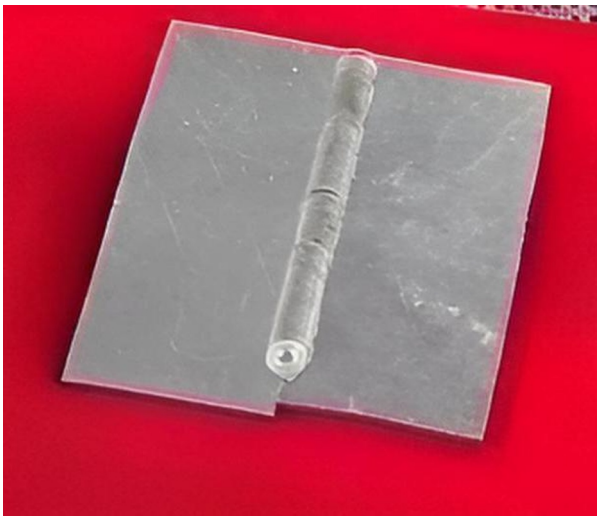

Fig.1. FSW sample

The nine distinct sample combinations produced by FSW were delineated follows and shown in Table 6.

Table 6: Material Combinations

Material Combination
AA 2024 with AA 3003
AA 2024 with AA 3003 + 5% TiC
AA 2024 with AA 3003 + 5% ZrC
AA 3003 with AA 2024 + 5% TiC
AA 3003 with AA 2024 + 5% ZrC
AA 2024 + 5% Al_2O_3 with AA 3003 + 5% TiC
AA 2024 + 5% Al_2O_3 with AA 3003 + 5% ZrC
AA 2024 + 5% ZrC with AA 3003 + 5% TiC
AA 2024 + 5% ZrC with AA 3003 + 5% ZrC

The parameters of the FSW process significantly affect morphological and mechanical qualities of weld. Therefore, enhancing them were feasible objective. Nevertheless, optimizing the FSW parameters for all nine aforementioned material combinations would need extensive testing. Utilizing DOE approaches, such as Box–Behnken and central composite, will still result in a substantial number of trials required to determine the best process parameters for all material combinations.

2.4 Optimization methodology

The optimization of FSW process was performed by MCDM approach, combining the CRITIC and MABAC methods [20]. The CRITIC method were used to calculate mass of criteria such as Brinell Hardness Number (BHN), corrosion resistance and Ultimate Tensile Strength (UTS), based on their standard deviation and inter – criteria correlation. Then the MABAC method ranked the alternatives by evaluating their proximity to the ideal solution. This approach provided a data – driven optimization techniques for selecting the best FSW combinations based on multiple criteria.

2.5. CRITIC technique

CRITIC is an objective weighting method used in decidion making.

Create a initial decision-making matrix:

$$X_{ij} = \begin{pmatrix} M_{11} & M_{12} & \dots & M_{1j} \\ M_{21} & & & \vdots \\ \vdots & & & \vdots \\ M_{i1} & \dots & \dots & M_{ij} \end{pmatrix}_{i \times j} \quad (1)$$

Where, m were number of options; n were number of criteria.

$$X_{ij} = \frac{A_{ij} - A_j^{\min}}{A_j^{\max} - A_j^{\min}}, \text{ if j} \in \text{beneficial attribute} \quad (2)$$

$$\mathrm{X}_{ij} = \frac{A_j^{\max} - A_{ij}}{A_j^{\max} - A_j^{\min}}, \text{ if j} \in \text{non - beneficial attribute} \quad (3)$$

Next, standard deviation (δ_j) were computed for all attribute as;

$$\delta_j = \sqrt{\frac{\sum_{i=1}^{h} (\mathrm{X}_{ij} - \Lambda_j)^2}{\hbar - 1}}; j = 1, \cdots, \lambda \quad (4)$$

Here, Λ_j were mean of j$^{\text{th}}$ attributes assumed by;

$$\Lambda_j = \frac{\sum_{i=1}^{n} \mathrm{X}_{ij}}{\hbar}; j = 1,2, \cdots \lambda \quad (5)$$

Correlation coefficient (ρ_{jk}) for all pair of attributes by following formula;

$$\rho_{jk} = \frac{\sum_{i=1}^{n} (\mathrm{X}_{ij} - \Lambda_j)(\mathrm{X}_{ik} - \Lambda_k)}{\sqrt{\sum_{i=1}^{n} (\mathrm{X}_{ij} - \Lambda_j)^2 \sum_{i=1}^{n} (\mathrm{X}_{ik} - \Lambda_k)^2}} \quad (6)$$

Mean of k -th attribute (Λ_k) were by Eqn. (16).

For all attribute, information measure (σ_j) value were computed as:

$$\sigma_j = \delta_j \sum_{k=1}^{\lambda} (1 - \rho_{jk}); j = 1, \cdots, \lambda \quad (7)$$

Objective weight (ω_j) of all attribute by CRITIC technique were determined as:

$$\omega_j = \frac{\sigma_j}{\sum_{j=1}^{\lambda} \sigma_j}; j = 1, \cdots, \lambda \quad (8)$$

2.6. MABAC method

The steps of MABAC method are listed below
Step 1: Calculate normalized values r_{ij}:

$$r_{ij}^* = \frac{X_{ij} - X_i^-}{X_i^+ - X_i^-}$$
$$r_{ij}^* = \frac{X_{ij} - X_i^+}{X_i^- - X_i^+} \quad (9)$$

In $j = 1,2, \ldots, n$ and$i = 1,2, \ldots, m$. Eqn (2) were for criteria MRR, and (3) were for creation SR and EWR.

Step 2: Find weighted matrix :

$$v_{ij} = w_j + w_j \times r_{ij}^* \quad (10)$$

Step 3: Calculate the border approximation area matrix:

$$g_j = \left(\prod_{i=1}^{m} v_{ij}\right)^{1/m} \quad (11)$$

Step 4: Determine distance among options and border approximation area by:

$$q_{ij} = v_{ij} - g_i \quad (12)$$

Step 5: Compute total distances at all option from border area:

$$S_i = \sum_{j=1}^{n} q_{ij} \quad (13)$$

Step 6 : Rank options by maximizing S_i.

3.Experimental Results

The assessment of the FSW process is performed by executing several experiments that illustrate distinct material behaviors. This research includes experiments to evaluate the mechanical characteristics, including tensile strength, hardness, and corrosion resistance, of various weld combinations including composites and alloys. The values derived from corrosion and mechanical testing were compared between weld samples to determine which combination yields the optimal results.

3.1. Mechanical Tests

This section encompasses tests conducted to ascertain Brinell Hardness Number (BHN) and ultimate tensile strength (UTS) of weld sample.

3.1.1. Tensile Test

This test assesses the material's ductility. Ductility is a property that allows material to be deformed into elongated and slender wire. Ductile materials like aluminium possesses more elasticity. The tensile test were performed at the tension chamber of a universal testing machine (UTM) located at Blue Star, Mumbai, India given in Table 7. FSW sample sectioned with various combinations and processed as shown in Fig 2. The test specimen were sequentially positioned among stationary jaw and a movable jaw of Universal Testing Machine (UTM). As the moveable jaw initiates vertical movement by hydraulic power, a tensile stress is exerted on the sample, causing it to elongate. Upon transitioning from the elastic to the plastic area, the sample absorbs maximal stress prior to fracture. The greatest alteration in length transpires after application of ultimate tensile stress or maximal load.

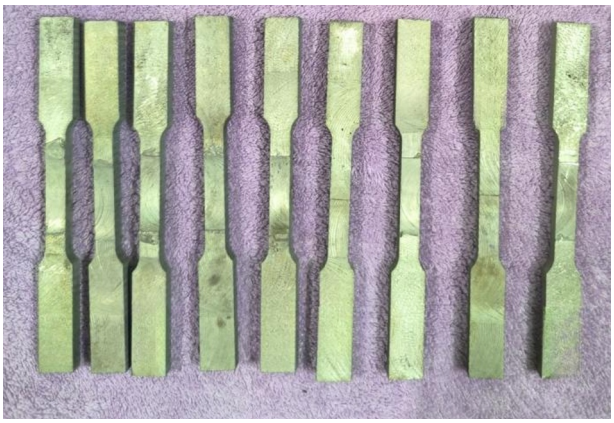

Fig. 2. Tensile test specimen

Table 7. Tensile test results

Specimen No.	Maximum Load	Cross-Section Area (bxt), A_o	UTS,	Elongation
1	4989	181.79	124.97	7
2	4282	161.33	106.42	7.7
3	3523	139.4	88.13	8.67
4	5650	197.99	140.82	6.55
5	3300	132.6	82.76	9.04
6	4464	166.68	111.12	7.5
7	3529	139.32	88.06	8.68
8	2986	121.45	74.25	9.73
9	4124	156.82	102.53	7.88

The findings demonstrate that FSW specimen 4, including AA3003 alloy welded with AA 2024/5% TiC composite has the best ultimate tensile strength (UTS). This signifies an impeccable link between the two plates at the weldment area. The frictional stir welding combination of AA 2024 alloy with AA 3003 alloy yields second highest score among combinations, since the alloy demonstrates high ductility than the composite. Welding combination of AA 2024/5% ZrC and AA 3003/5% TiC exhibits the lowest tensile strength

because to the brittleness induced by the presence of both ceramics, resulting in a weakened FSW bond. In prior research, friction stir welding of AA2024 and AA356-T3 alloys optimized the mechanical properties, increasing tensile strength and hardness while maintaining corrosion resistance, highlighting its potential for durable aluminum matrix composites [21]. The FSW combinations that include ZrC exhibit diminished tensile strength because to ZrC's superior hardness compared to TiC.

3.1.2. Hardness Test

This test measures hardness of sample by computing the Brinell Hardness Number. Hardness refers to degree to material can endure abrasion or indentation forces, is given in Table 8. The samples were positioned horizontally at hardness tester, allowing point stress of 250 kgf to be exerted on weldment surface with a diameter of 5 mm, maintained for a duration of 10 seconds. The BHN were derived from Equation (15).

$$\text{BHN} = \frac{2P}{\pi D\left[D-\sqrt{D^2-d^2}\right]} \quad (15)$$

Where

P =constant load (250 kgf);

D =diameter (5 mm);

d =diameter in mm

The results clealry demonstrate that FSW AMC exhibit greater hardness than FSW aluminum alloy. The incorporation of ZrC significantly enhances hardness compared to TiC. Alloy weld combination had lowest hardness, whereas ZrC-reinforced composite weld combination demonstrates the highest hardness. Reinforcement of AA7075 and AA2024 FSW joints with SiC and TiO_2 nanoparticles enhances microstructure, hardness, and tensile strength, with SiC showing the highest tensile strength improvement [22].

Table 8. Hardness results

Specimen No.	Diameter of Impression	Brinell Hardness
1	3.82	47.41
2	3.68	50.64
3	3.51	55.41
4	3.56	53.28
5	3.46	56.26
6	3.53	54.51
7	3.39	58.41
8	3.42	57.5
9	3.32	60.84

3.2. Corrosion Test

Corrosion is the process of bulk material degradation. The corrosion test were conducted to determine which sample exhibits the highest corrosion resistance between various

combinations. In prior research, multi-pass FSP of AA2024 with AlB_2 reinforcement improves microstructure, hardness, and wear resistance, showcasing enhanced mechanical properties and corrosion resistance in aluminum matrix composites [23]. Test, specimen were extracted from nine weld combinations, ensuring that weldment zone is positioned among samples and were prepared. The samples were individually submerged at alkaline and acid solutions for a duration of 24 hours. The samples are then removed, and mass loss attributable to corrosion were determined by calculating difference among the initial weight of specimen prior to immersion in the corrosive liquid and the final weight following extraction from medium. Corrosion rate were ultimately determined using the formula specified at Eqn (16):

$$CR = \frac{87.6W}{\rho AT} \quad (16)$$

Where,

CR = corrosion rate
ρ = density
W = mass loss
T = exposure
A = cross-sectional area

The corrosion rate unit were converted to mpy via Equation (17) shown below.

$$1\text{mpy} = 0.0254\text{mm/y} \quad (17)$$

A reduced corrosion rate indicates an enhanced corrosion resistance of weld sample. Table 9 illustrates corrosion rates of sample submerged at acidic and basic environments.

Table 9. Test results of Immersion corrosion

Specimen No.	CR_A		CR_B	
	Acid Solution		Base Solution	
	mm/y	Mpy	mm/y	mpy
1	21.1	0.83	36.8	1.45
2	15	0.59	21.1	0.83
3	17.3	0.68	25.1	0.99
4	13.2	0.52	20.3	0.8
5	16	0.63	22.4	0.88
6	10.9	0.43	14.5	0.57
7	11.7	0.46	15.5	0.61
8	12.5	0.49	18.8	0.74
9	14.5	0.57	20.3	0.8

The conclusions derived from the aforementioned test findings unequivocally indicate that composite-composite weld and alloy-composite combinations provide superior corrosion resistance compared to the alloy-alloy combination. Composite–composite weld outperform the alloy–composite combinations. The incorporation of titanium carbide is essential for decreasing corrosion rate at welded samples. The sample with titanium carbide exhibit superior corrosion resistance compared to those with zirconium carbide.

3.3. Optimal Frictional Stir Welding Combination by CRITIC – MABAC

Table 10 presents the choice matrix established for the aforementioned research study.

Table 10. Decision matrix.

Sample	Ultimate tensile strength	BHN	CR_A (mpy)	CR_B (mpy)
1	124.97	47.41	0.83	1.45
2	106.42	50.64	0.59	0.83
3	88.13	55.41	0.68	0.99
4	140.82	53.28	0.52	0.80
5	82.76	56.26	0.63	0.88
6	111.12	54.51	0.43	0.57
7	88.06	58.41	0.46	0.61
8	74.25	57.5	0.49	0.74
9	102.53	60.84	0.57	0.79

3.3.1. CRITIC weighting method

The CRITIC weighting approach, constructed decision matrix were normalized. Investigated in previous research, CRITIC-BPNN method optimizes FSW process parameters for AA6082-T6, with welding speed identified as the most influential factor, providing accurate predictions for tensile strength and elongation [24] is in Table 11. The correlation coefficient ρ_{jk}information measure σ_j and standard deviation $\delta_j$values was obtained by Eq. (15)-18).

Table 11. CRITIC results

	UTS	Hardness	CR_A	CR_B
Wj	0.255	0.374	0.192	0.179

Weight of attribute Hardness (0.374) were found to maximum followed by UTS (0.255) and AcidicCorrosion Rate solution ($CR_{A)}$ (0.192) whereas, it remains lowest for Basic Corrosion Rate Solution($CR_{B)}$ (0.179).

3.3.2. MABAC for alternative ranking

The stages for carrying out MCDM using the MABAC technique detailed and Initial matrix were generated in accordance with Eqn (1). Subsequently, Eqn (2), pertaining to UTS and BHN objective, and (3), associated with the CR_A and CR_B objectives, will be employed calculate normalized values of r_{ij} * displayed in Table 12. Normalized weighted values, denoted as v_{ij}, were subsequently calculated utilizing formula (4) are shown in Table (12).

Table 12. Normalized and weighted normalized decision matrix

S.No	UTS	Hardness	CR_A	CR_B	UTS	Hardness	CR_A	CRB
	Normalized Decision Matrix				Weighted Normalization			
1	0.7619	0.0000	0.0000	0.0000	0.4493	0.3740	0.1920	0.1790
2	0.4833	0.2405	0.6000	0.7045	0.3782	0.4639	0.3072	0.3051

3	0.2085	0.5957	0.3750	0.5227	0.3082	0.5968	0.2640	0.2726
4	1.0000	0.4371	0.7750	0.7386	0.5100	0.5375	0.3408	0.3112
5	0.1278	0.6590	0.5000	0.6477	0.2876	0.6205	0.2880	0.2949
6	0.5539	0.5287	1.0000	1.0000	0.3962	0.5717	0.3840	0.3580
7	0.2075	0.8191	0.9250	0.9545	0.3079	0.6803	0.3696	0.3499
8	0.0000	0.7513	0.8500	0.8068	0.2550	0.6550	0.3552	0.3234
9	0.4248	1.0000	0.6500	0.7386	0.3633	0.7480	0.3168	0.3112

The matrix representing the border approximation area is computed utilizing Equation (5) are shown in Table 13.

Table 13. Border Area Matrix

	UTS	**Hardness**	**CR_A**	**CR_B**
Gi	0.354	0.5722	0.307	0.296

The computation of distance among alternatives and boundary approximation area q_{ij} were executed utilizing formula (6). Ultimately, comprehensive distances among all alternative and projected border area S_i were ascertained utilizing formula (7). In order to ascertain ranking of the alternatives, S_i were subjected to refinement. Table 14 presents a variety of computed parameters in conjunction with the ranking of alternatives derived from the MABAC method. In previous studies, MABAC method in a neutrosophic fuzzy environment optimizes FSW processes for AA2024, achieving optimal parameter combinations and demonstrating the effectiveness of the hybrid MCDM approach in improving weld quality and efficiency [25].

Table 14. Border approximation area (q_{ij}), total Distance (S_i) and Final Ranking

S.No	**UTS**	**Hardness**	**CR_A**	**CR_B**	**Si**	**Rank**
1	0.096	-0.1982	-0.115	-0.117	-0.3346	9
2	0.024	-0.1083	-1E-04	0.01	-0.0744	7
3	-0.046	0.0245	-0.043	-0.023	-0.0874	8
4	0.156	-0.0348	0.034	0.016	0.1706	4
5	-0.066	0.0482	-0.019	-6E-04	-0.0379	6
6	0.043	-0.0005	0.077	0.062	0.1811	2
7	-0.046	0.1081	0.062	0.054	0.1788	3
8	-0.099	0.0827	0.048	0.028	0.0597	5
9	0.01	0.1758	0.01	0.016	0.2105	1

Based on data at Table 14, it is observed that 9th run is the most beneficial.

Attribute of ideal FSW combination were presented at Table 15 below. The aforementioned table indicates that FSW specimen 6, including AA2024/5%, TiC, O-3. coupled with AA3003/5%, TiC, O-3., represents the optimal combination.

Table 15. Optimized FSW specimen.

MABAC, Si	Rank	Sample	UTS (MPa)	BHN	CR_A (mpy)	CR_B (mpy)
0.2105	1	9	102.53	60.84	0.57	0.8

4. Conclusions

Aluminum alloys are widely utilized in many applications that need a high strength-to-weight, low mass, exceptional thermal characteristics, and superior surface quality. Researchers were primarily investigating Aluminum Matrix because of its superior chemical, tribological and mechanical qualities. The assessment of corrosion resistance and mechanical characteristics through comparative analysis to examine the FSW process regarding the joining of different AMC and Al alloys. Conclusions can be derived through experimental research.

Ultimate Tensile Strength (UTS): The highest UTS of **124.97 MPa** was observed in the combination of AA3003 alloy welded AA2024/5% TiC, while lowest UTS of**102.53 MPa** was found in the combination of AA2024/5% ZrC welded with AA3003/5% TiC. This indicates that the presence of ceramics like SiC can induce brittleness and weaken the weld.

Hardness (BHN): The highest Brinell Hardness Number (BHN) of **60.84** was recorded for the combination of AA3003/5% ZrC welded with AA2024/5% ZrC, which indicates improved hardness due to the ZrC reinforcement.

Corrosion Resistance: The **acidic corrosion rate (CR_A)** of the best performing specimen, AA2024/5% TiC welded with AA3003/5% TiC, was as low as **0.8 mm/y**, and the **basic corrosion rate (CR_B)** was **0.57 mpy**, indicating superior corrosion resistance compared to other combinations.

MABAC and **CRITIC Optimization**: The **MABAC** and **CRITIC** method was successfully implemented, identifying the combination of AA2024/5% TiC welded with AA3003/5% TiC as good solution. This combination achieved highest **MABAC** and **CRITIC coefficient** of **0.01.**

A limitation of study were the exclusive consideration of aluminum and composites. The research may be enhanced by incorporating various FSW process parameters and diverse compositions. The application of contemporary multicriteria decision-making approaches like SECA and CoCoSo along with global optimization techniques, may enhance the ideal answer.

References

[1] A. A. Barakat, A. A. Ahmed, B. M. Darras, and M. A. Nazzal, "Towards Sustainable Metal-to-Polymer Joining: A Comparative Study on Friction Stir Welding, Self-Piercing Riveting, and Adhesive Bonding," Sustainability (Switzerland), vol. 16, no. 9, (2024), doi: 10.3390/su16093664.

[2] M. Milčić, D. Klobčar, D. Milčić, N. Zdravkovic, A. Duric, and T. Vuherer, "Comparison between Mechanical Properties and Joint Performance of AA 2024-T351 Aluminum Alloy Welded by Friction Stir Welding, Metal Inert Gas and Tungsten Inert Gas Processes," Materials, vol. 17, no. 13, (2024), doi: 10.3390/ma17133336.

[3] S. S. Baghel and P. K. Kumar Soni, "Mechanical and metallurgical characterization of friction stir welded AA2024 to pure copper using specific variables and positioning," Proc. Inst. Mech. Eng. C J. Mech. Eng. Sci., vol. 238, no. 11, pp. 5014–5025, (2024), doi: 10.1177/09544062231217610.

[4] A. Sharma, Z. A. Khan, A. N. Siddiquee, and M. Arif, "Study of friction stir welding effects on the microstructure & mechanical properties of AA3003 pipes," Phys. Scr., vol. 100, no. 1, (2025), doi: 10.1088/1402-4896/ad9ee4.
[5] A. K. Choudhary and R. Jain, "Process mechanics and flow stream investigation during FSW of thick AA2024 plate by eccentric square pin," Mater. Chem. Phys., vol. 345, (2025), doi: 10.1016/j.matchemphys.2025.131239.
[6] M. Naseri, M. Alvand, O. Imantalab, D. Gholami, and E. Borhani, "EFFECT OF POST-WELD HEAT TREATMENT ON TENSILE PROPERTIES OF FRICTION STIR-WELDED JOINTS OF NANOSTRUCTURED AA2024 ALLOY," Journal of Chemical Technology and Metallurgy, vol. 60, no. 5, pp. 791–798, (2025), doi: 10.59957/jctm.v60.i5.2025.10.
[7] B. Krishna, G. Mrudula, Y. Yanda, P. Prakash, D. V Janaki, and M. V. N. V. Satyanarayana, "Mechanical Properties Enhancement in Friction Stir Processed AA2024 Alloy through Pin Profile Optimization," Journal of The Institution of Engineers (India): Series D, vol. 106, no. 2, pp. 1221–1233, (2025), doi: 10.1007/s40033-024-00751-3.
[8] S. Xing, J. Sun, C. Zhang, H. Shou, L. Jia, and N. Lv, "Effect of joining material direction on material flow, microstructure and mechanical properties of dissimilar AA2024/7075 joints fabricated by friction stir welding," Journal of Materials Research and Technology, vol. 35, pp. 3679–3692, (2025), doi: 10.1016/j.jmrt.2025.02.007.
[9] F. A. Mir, N. Z. Khan, K. A. Sheikh, I. A. Badruddin, and S. Kamangar, "Performance analysis of Al stainless steel joints fabricated by friction stir welding: Microstructure, mechanical, and tribology," Proceedings of the Institution of Mechanical Engineers, Part J: Journal of Engineering Tribology, vol. 238, no. 10, pp. 1234–1246, (2024), doi: 10.1177/13506501241246841.
[10] H. Kheirabadi, B. Beidokhti, S. Khadivi, and A. Davodi, "Investigation on Microstructure and Residual Stress Distribution in Dissimilar AA3105/AA2024 Friction Stir Joints," J. Mater. Eng. Perform., vol. 33, no. 15, pp. 7763–7769, (2024), doi: 10.1007/s11665-024-09681-3.
[11] H. Jamshidi Aval, "Effect of heat input in dissimilar friction stir welding of A390-10 wt.% SiC composite–AA2024 aluminum alloy," Archives of Civil and Mechanical Engineering, vol. 24, no. 3, (2024), doi: 10.1007/s43452-024-00957-y.
[12] I. Chekalil et al., "Effect of corrosion environments on the mechanical properties of friction stir welded aluminum alloy AA3003," Journal of Materials Research and Technology, vol. 33, pp. 2353–2364, (2024), doi: 10.1016/j.jmrt.2024.09.167.
[13] I. Chekalil, R. Chadli, A. Ghazi, A. Miloudi, M.-P. Planche, and A. Amrouche, "Corrosion behavior of AA3003 friction stir welded joints," Colloids Surf. A Physicochem. Eng. Asp., vol. 680, 2024, doi: 10.1016/j.colsurfa.(2023).132673.
[14] P. P. Das and S. Chakraborty, "In search of the best multi-criteria decision making-particle swarm optimization-based hybrid approach for parametric optimization of friction stir welding processes," OPSEARCH, vol. 61, no. 4, pp. 1764–1794, (2024), doi: 10.1007/s12597-024-00757-1.
[15] A. Kumari and B. Acherjee, "A novel hybrid multi-criteria decision methodology for assessing tool materials in friction stir welding process," International Journal on Interactive Design and Manufacturing, vol. 18, no. 7, pp. 4963–4986, (2024), doi: 10.1007/s12008-024-01783-5.
[16] A. P. Edlabadkar, B. Mudadla, K. Karthick, M. S. Kumar, A. Adams, and M. Selvaraju, "Optimization of Machining Parameters and Performance Analysis of AA2024/ZrO2 Metal Matrix Composite Using TOPSIS: Insights into Squeeze Casting and Tribological Behavior," Journal of Environmental Nanotechnology, vol. 14, no. 1, pp. 181–192, (2025), doi: 10.13074/jent.2025.03.2441016.

[17] V. Viswanathan, A. K. Babuchellam, V. Vimala, and M. Selvaraju, "Optimizing underwater friction-stir welding parameters for AA356/SiC composites using CoCoSo and MEREC: enhancing joint performance and quality," Revista Materia, vol. 30, (2025), doi: 10.1590/1517-7076-RMAT-2024-0948.
[18] R. Srinivasan et al., "Investigation on the Mechanical Properties of Powder Metallurgy-Manufactured AA7178/ZrSiO4Nanocomposites," Advances in Materials Science and Engineering, vol. (2023), 2023, doi: 10.1155/2023/3085478.
[19] D. Dinesh Kumar et al., "Study of Microstructure and Wear Resistance of AA5052/B4C Nanocomposites as a Function of Volume Fraction Reinforcement to Particle Size Ratio by ANN," J. Chem., vol. 2023, (2023), doi: 10.1155/2023/2554098.
[20] I. Solomon, P. Sevvel, J. Gunasekaran, and J. Vasanthe Roy, "OPTIMIZING FSW PARAMETERS FOR AZ31B-AA6082 ALLOYS USING HYBRID MCDM AND MULTI-OBJECTIVE RSM MODELS: A NUMERICAL DECISION-MAKING APPROACH," Surface Review and Letters, (2025), doi: 10.1142/S0218625X25500994.
[21] I. Sabry, "Exploring the effect of friction stir welding parameters on the strength of AA2024 and A356-T6 aluminum alloys," Journal of Alloys and Metallurgical Systems, vol. 8, (2024), doi: 10.1016/j.jalmes.2024.100124.
[22] P. K. Mouria, R. M. Singari, and R. Wattal, "Microstructural and mechanical response of SiC and TiO2 particles reinforced friction stir welded AA7075 and AA2024," International Journal on Interactive Design and Manufacturing, vol. 18, no. 3, pp. 1331–1343, (2024), doi: 10.1007/s12008-023-01667-0.
[23] M. Nikzad-Dinan, R. Jamaati, and H. Jamshidi Aval, "Enhanced microstructure, strength, and wear resistance of AA2024-AlB2 composites via multi-pass friction stir processing," Journal of Materials Research and Technology, vol. 36, pp. 4293–4307, (2025), doi: 10.1016/j.jmrt.2025.04.043.
[24] M. A. Abolarin et al., "A CRITIC-BPNN APPROACH TO FRICTION STIR WELDING PARAMETRIC SELECTION AND PREDICTION USING AA6082-T6 MATERIAL," Kufa Journal of Engineering, vol. 16, no. 1, pp. 421–449, (2025), doi: 10.30572/2018/KJE/160123.
[25] S. Chatterjee and S. Chakraborty, "Optimization of friction stir welding processes using multi-attributive border approximation area comparison (MABAC) method in neutrosophic fuzzy environment," International Journal on Interactive Design and Manufacturing, vol. 17, no. 4, pp. 1979–1994, (2023), doi: 10.1007/s12008-023-01308-6.